Electrochemistry Hot Paper

Deutsche Ausgabe: DOI: 10.1002/ange.201707840
Internationale Ausgabe: DOI: 10.1002/anie.201707840

An Ultraflexible Silicon–Oxygen Battery Fiber with High Energy Density

*Ye Zhang, Yiding Jiao, Lijun Lu, Lie Wang, Taiqiang Chen, and Huisheng Peng**

Abstract: *To satisfy the rapid development of portable and wearable electronics, it is highly desired to make batteries with both high energy densities and flexibility. Although some progress has been made in recent decades, the available batteries share critical problems of poor energy storage capacity and low flexibility. Herein, we have developed a silicon–oxygen battery fiber with high energy density and ultra-high flexibility by designing a coaxial architecture with a lithiated silicon/carbon nanotube hybrid fiber as inner anode, a polymer gel as middle electrolyte and a bare carbon nanotube sheet as outer cathode. The fiber showed a high energy density of 512 Wh kg^{-1} and could effectively work after bending for 20000 cycles. These battery fibers have been further woven into flexible textiles for a large-scale application.*

Portable and wearable electronic devices have attracted increasing attention during recent decades,[1,2] because flexible power systems such as batteries play a critical role for developing high-performance electronic devices. Although great achievements have been made for developing various matching batteries, they face several common bottlenecks. The available flexible batteries are typically made in a sandwich-like film that has to be as thin as possible.[3–6] The flexibility is generally realized at the expense of sacrificing electrochemical properties, for example, a low loading of active materials was required, which largely reduced their energy densities.[7] In addition, the slip of two thin electrodes may produce short circuits under deformation.[8] Furthermore, they can bear some gentle deformations such as bending but may break under dramatic deformations including twisting and tying.[9,10] To this end, two-fiber electrodes were recently twisted together to form a new structure of thin lithium-ion batteries that were expected to display higher flexibility.[11–13] Unfortunately, on the one hand, much low energy densities were produced from the above twisted batteries.[13] On the other hand, the two-fiber electrodes tended to separate to largely decrease the electrochemical property and stability under severe or repeating deformations.[12] Development of appropriate batteries with both high energy densities and flexibility is urgent and remains challenging too.

Herein, we have discovered a silicon–oxygen battery (SOB) fiber with high energy density and ultra-high flexibility by designing a solid-state coaxial architecture with the lithiated silicon/carbon nanotube (CNT) hybrid fiber as inner anode, a polymer gel as middle electrolyte and a bare CNT sheet as outer cathode (Figure 1a). The full SOB fiber exhibited an energy density of 512 Wh kg^{-1} based on the total weight of the two electrodes. The as-fabricated lithiated silicon/CNT hybrid fiber not only avoided dendrite formation and the safety issue of lithium metal[14,15] but also showed ultra-high flexibility. The SOB fiber could effectively work after 20000 bending cycles. As expected, the fiber shape enabled it to be woven into flexible textiles for a large-scale application.

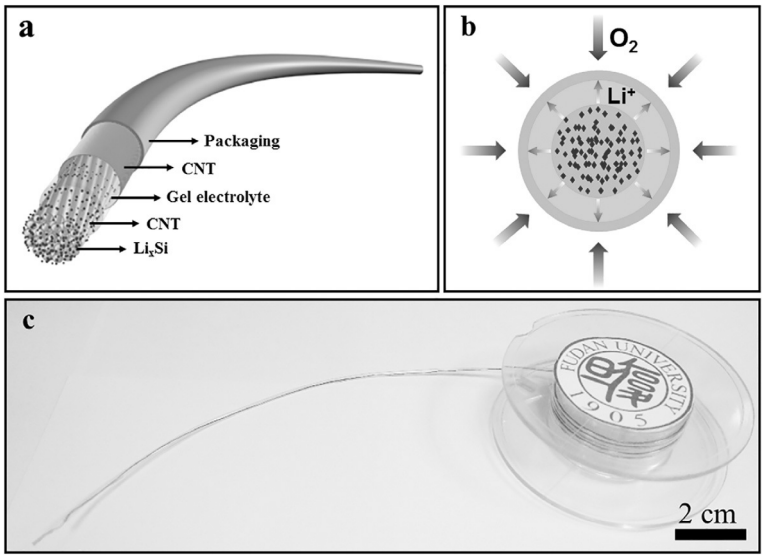

Figure 1. a,b) Schematic illustration to the structure and working mechanism of an SOB fiber, respectively. c) Photograph of an SOB fiber.

The Si nanoparticles were first coated onto aligned CNT sheets and then continuously co-spun to produce silicon/CNT hybrid fibers. After a lithiation process through an electrochemical reaction, the lithiated silicon/CNT fiber anode was

[*] Y. Zhang, Y. Jiao, L. Wang, Dr. T. Chen, Prof. H. Peng
State Key Laboratory of Molecular Engineering of Polymers
Department of Macromolecular Science and
Laboratory of Advanced Materials, Fudan University
Shanghai 200438 (China)
E-mail: penghs@fudan.edu.cn
L. Lu
College of Materials Science and Engineering and
The Key Laboratory of Material Processing and
Mold of Ministry of Education, Zhengzhou University
Zhengzhou (China)

Supporting information for this article can be found under: https://doi.org/10.1002/anie.201707840.

obtained. The resulting fiber anode was then coated with a layer of polymer gel electrolyte. The electrolyte was a mixture of bis(trifluoromethane sulfonimide) (LiTFSI), lithium nitrate ($LiNO_3$), tetraglyme, poly(vinylidene fluoride-co-hexafluoropropylene) (PVDF-HFP), *N*-methyl-2-pyrrolidinone (NMP), 2-hydroxy-2-methyl-1-phenyl-1-propanone (HMPP), and trimethylolpropane ethoxylate triacrylate (TMPET). The details are described in the Experimental Section.[16] The electrolyte showed a high ionic conductivity of 2.01 mS cm and could also effectively protect lithiated silicon/CNT fiber from corrosion by oxygen and water vapor in air. The CNT sheet was then wrapped evenly around the electrolyte to serve as the cathode. A punched heat-shrinkable tube was finally packed around the full battery for further protection (see Figure S1 in the Supporting Information).

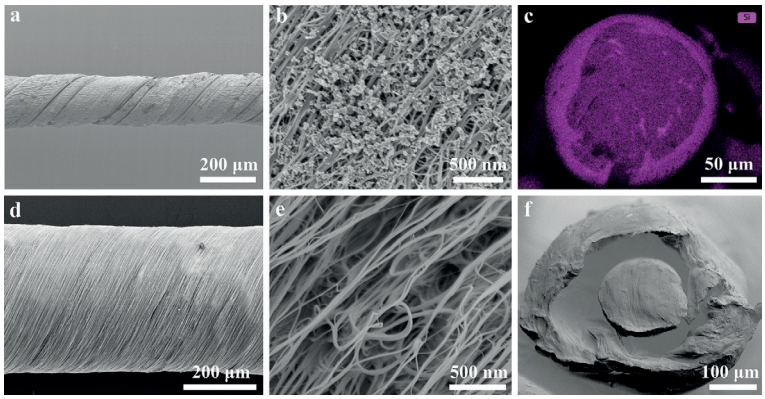

Figure 2. a,b) Scanning electron microscopy (SEM) images of silicon/CNT hybrid fiber at low and high magnifications, respectively. c) Energy-dispersive X-ray spectroscopy images by cross-sectional view of silicon/CNT hybrid fiber. Here silicon is marked with purple. d,e) SEM images of an SOB fiber at low and high magnifications, respectively. f) Cross-sectional SEM image of the SOB fiber.

The working principle of the SOB is shown in Figure 1b. During the discharge process, lithium ions dealloyed from the inner lithiated silicon/CNT fiber, and then transferred through the gel electrolyte. Oxygen diffused into the voids of aligned CNT sheets from all directions and reacted with lithium ions to form lithium peroxide (Li_2O_2) at the CNT cathode, while the electrons flowed from the anode to the cathode through the external circuit. The process was reverse during the charge process. The Reaction at the cathode is given in Equation (1).

$$x\,O_2 + 2x\,Li^+ + 2x\,e^- \underset{\text{charge}}{\overset{\text{discharge}}{\rightleftharpoons}} x\,Li_2O_2 \qquad (1)$$

The reaction at the anode is given in Equation (2).

$$2\,Li_xSi \underset{\text{charge}}{\overset{\text{discharge}}{\rightleftharpoons}} 2\,Si + 2x\,Li^+ + 2x\,e^- \qquad (2)$$

The coaxial structure facilitated the diffusion of ions and oxygen molecules in all directions while maintaining the integrality during deformation. This SOB fiber was thin with a diameter of 500 μm and highly flexible, which was beneficial for the weaving process later (Figure 1c).

Scanning electron microscopy (SEM) images of the silicon/CNT hybrid fiber are shown in Figures 2a–c. The hybrid fiber showed a uniform diameter of approximately 160 μm, and the CNTs were highly aligned along the axial direction, thus providing both high tensile strengths (10^2 to 10^3 MPa) and electrical conductivities (10^2 to 10^3 S cm). Therefore, the aligned CNTs can effectively serve as skeletons for incorporation of active nanoparticles and continuous electron pathways. Si nanoparticles with diameters of 50 nm were uniformly dispersed in the hybrid fiber with numerous voids among them (Figures 2b and S2), and the energy-dispersive X-ray mapping of Si by cross-sectional view further verified the distribution state (Figure 2c). The linear density of the hybrid fiber was 0.023 mg cm^{-1} and the thermogaravimetric analysis shows the content of silicon nanoparticles in weight was 83.84 % (Figure S3), which can be controlled by varying the concentration

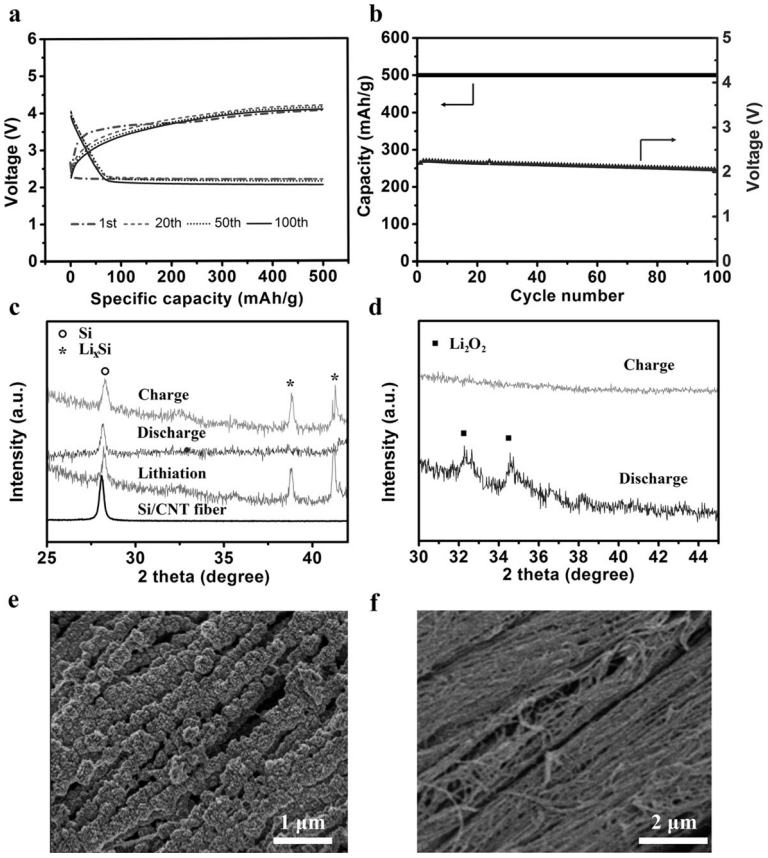

Figure 3. a,b) Charge and discharge curves and the corresponding cycling performance of the SOB fiber, respectively. c,d) X-ray diffraction patterns of the anode and cathode at different states, respectively. e,f) SEM images of the CNT cathode after the first discharge and first recharge, respectively.

of silicon slurry. After a lithiation process, the hybrid fiber was coated with gel electrolyte and finally wrapped by a lay of CNT sheets. The SOB fiber showed a uniform diameter of 400 μm (Figure 2d). The outer CNT sheet was also highly aligned along the axial direction. The specific surface area was 84.79 $m^2 g^{-1}$ (Figure S4) and the formed nanosized voids facilitated the diffusion of O_2 (Figure 2e). The core–shell structure of the SOB fiber was further verified by cross-sectional SEM image (Figure 2f).

Before assembling into an SOB full battery, the electrochemical performances of inner anode fiber and outer CNT cathode were first investigated in half-cells with lithium as the counter electrode. Figure S5 shows the charge and discharge curves of the lithiated silicon/CNT hybrid fiber anode. The fiber electrode exhibited an average discharge voltage of around 0.3 V and a fully reversible capacity of 1250 mAh g^{-1} at the current of 0.1 mA. After 100 charge and discharge cycles, the capacity was maintained by above 80% (Figure S6). The excellent cycling performance was derived from the unique design of the electrode. The spiral structure enabled a firm combination of the active nanoparticles on the CNTs, and the numerous voids provided space for volume expansion. The performance of the aligned CNT cathode was also carefully studied. The cathode showed an average discharge voltage of 2.5 V with a cutoff capacity of 500 mAh g^{-1} at a current of 0.1 mA (Figure S7). Besides, the capacity was well maintained and the average discharge voltage remained almost unchanged after 100 charge and discharge cycles (Figure S8). The voltage difference and the stable electrochemical properties of the two electrodes made them suitable for constructing metallic lithium-free full batteries.

The lithiated silicon/CNT hybrid fiber anode and aligned CNT cathode were assembled into a coaxial structure with gel electrolyte between them to form the SOB fiber with length of 8 cm and internal resistance of 253 Ω (Figure S9). The galvanostatic charge and discharge measurement was conducted in Figure 3a. The SOB fiber showed an average discharge voltage of 2.1 V with a capacity cutoff of 500 mAh g^{-1}. The corresponding capacity and discharge voltage remained almost unchanged after 100 cycles, indicating that the battery can be steadily used for more than 100 cycles (Figure 3b). Based on the total mass of the two electrodes, the energy density was calculated as 512 Wh kg^{-1}.

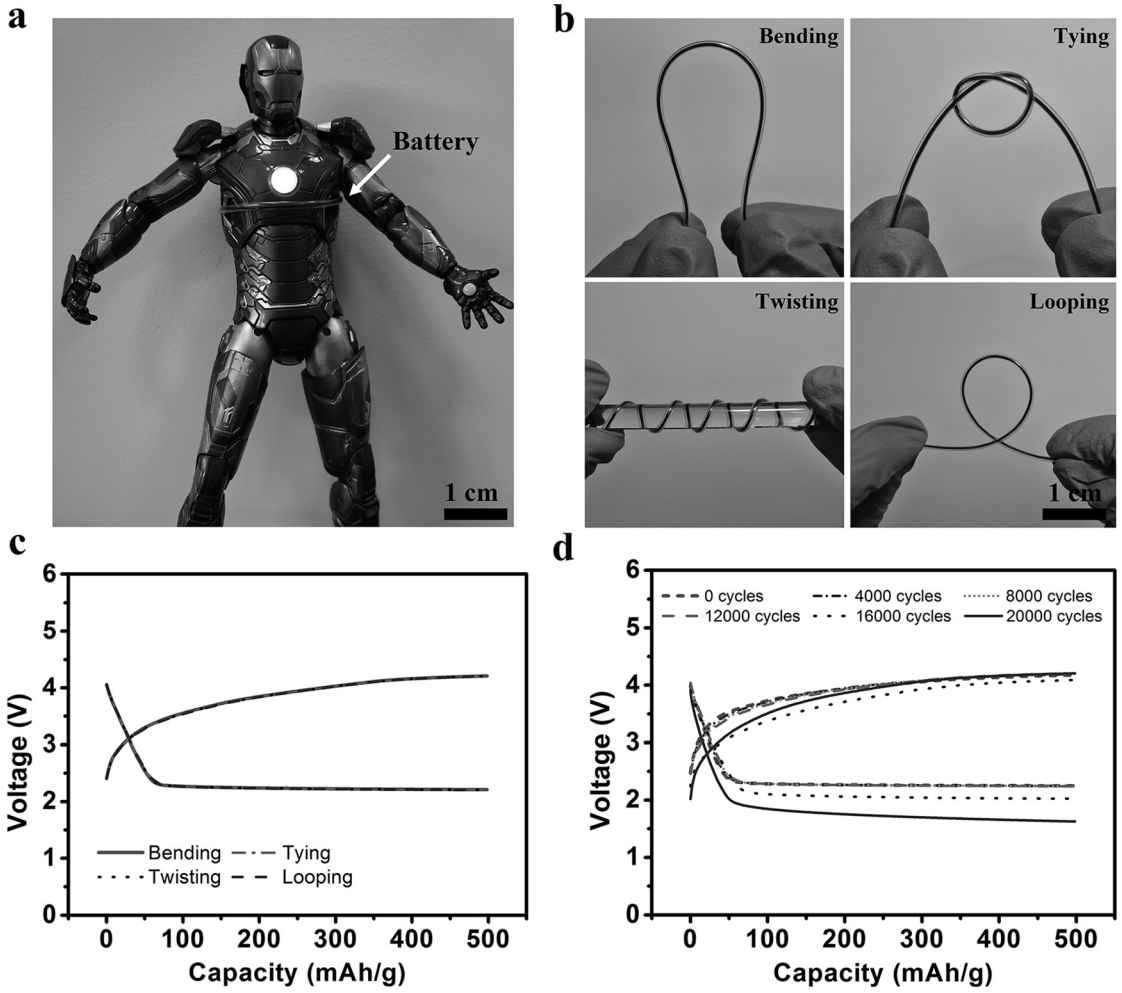

Figure 4. a) A bent SOB fiber lighting up a light-emitting diode (LED). b) An SOB fiber under various deformations. c) Charge and discharge curves of the SOB fiber under various deformations. d) Charge and discharge curves of the SOB fiber before and after different bending cycles. For a typical bending test, the SOB fiber with length of 8 cm was bent into circle with the distance between two ends as 1 cm.

The reversibility of the lithiated silicon/CNT fiber anode was confirmed by X-ray diffraction (XRD) analysis (Figure 3c). The characteristic peak of 28.0° related to Si was observed for the nonlithiated silicon fiber. After lithiation, the characteristic peaks of 38.7° and 41.5° appeared, suggesting the formation of Li_xSi.[17] The characteristic peak of Si decreased, indicating that Si was predominant relative to a small amount of nonlithiated Si. The reversibility feature had been observed during the later discharge/charge process. After discharging, the characteristic peaks attributing to Li_xSi vanished, while after the sequential charge process, these peaks appeared again. These results verify the authenticity of the reversible reaction at the anode.

The reaction products of the SOB fiber on the CNT cathode after discharging and recharging processes were investigated by XRD (Figure 3d) and SEM (Figure 3e, f). The characteristic peaks of 32.3° and 34.7° related to Li_2O_2 were observed after the discharge process, and the peaks all vanished after the following recharge process.[18] These results demonstrated the main reaction product of Li_2O_2, high reversibility during recharging, and formation/disappearance of Li_2O_2 at the cathode. The above phenomena had been further verified by SEM. After discharging at a current of 0.1 mA, some nanoparticles with an average diameter of around 300 nm appeared on the CNT electrode; they all decomposed after the later recharging process. These observations further confirmed the reactions given in Equations (1) and (2).

The SOB fiber effectively powered an light-emitting diode (LED) under bending (Figure 4a). The SOB fiber could also bear multiple deformations including bending, tying, twisting and looping (Figure 4b), which showed its ultra-high flexibility. Under such deformations, the charge and discharge behaviors of the SOB fiber showed no significant changes (Figure 4c). The voltage profiles were perfectly maintained even after repeating the bending tests for 20000 cycles (Figure 4d), indicating a long-term stability under repeated deformations. The ultra-high flexibility can be attributed to two main factors. 1) No metal current collector and metallic lithium anode were used, and the use of aligned CNTs as both cathode and anode effectively increased the elasticity, which offered intrinsic flexibility for the SOB fiber. 2) The coaxial structure of the SOB fiber ensured the high integrity of each component of the SOB and a close fit of the layers, avoiding stress concentration with better flexibility.

The energy storage capacity and flexibility are two key parameters for the battery application. Figure 5 summarizes and compares this ultraflexible SOB fiber and the previous flexible batteries in energy density and bending cyclic stability.[3,12,13,19–24] The SOB shows a high energy density that is 2 to 10 times higher than that of the other flexible batteries. It can also bear 20000 bending cycles. The cycle number has been greatly improved by 10 to 100 times compared to other flexible batteries.

The SOB fiber can be continuously fabricated and woven into multiple flexible structures such as textiles (Figure 6a). The resulting textile can bear various deformations such as bending, folding and twisting (Figure 6b and c). After fabrication of a wristband, the SOB textile can effectively power a commercial LED screen (Figure 6d).

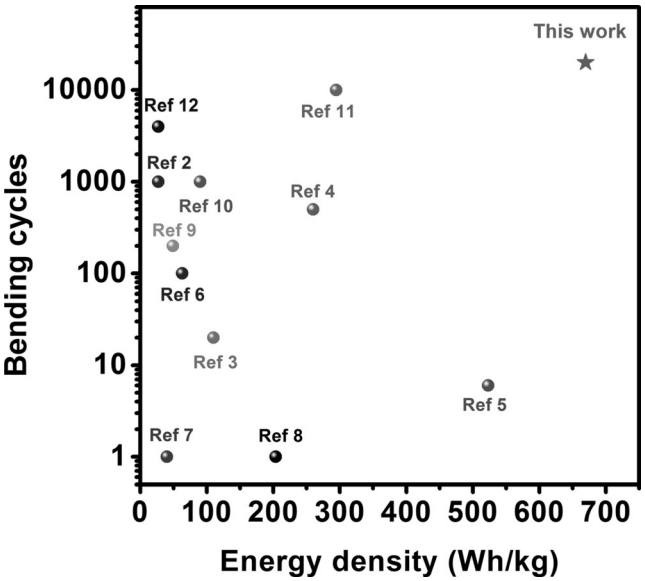

Figure 5. Energy density and bending cyclic stability of the ultraflexible SOB fiber compared with the previous energy storage systems including a lithium-ion battery (LIB) fiber,[12] LIB film,[3] sodium-ion battery tube,[24] aqueous LIB film,[19] Al-ion battery,[20] Sony Li-ion polymer battery, aqueous LIB fiber,[13] hybrid battery fiber,[23] Li–O_2 battery film,[22] and Li–O_2 battery cable.[21]

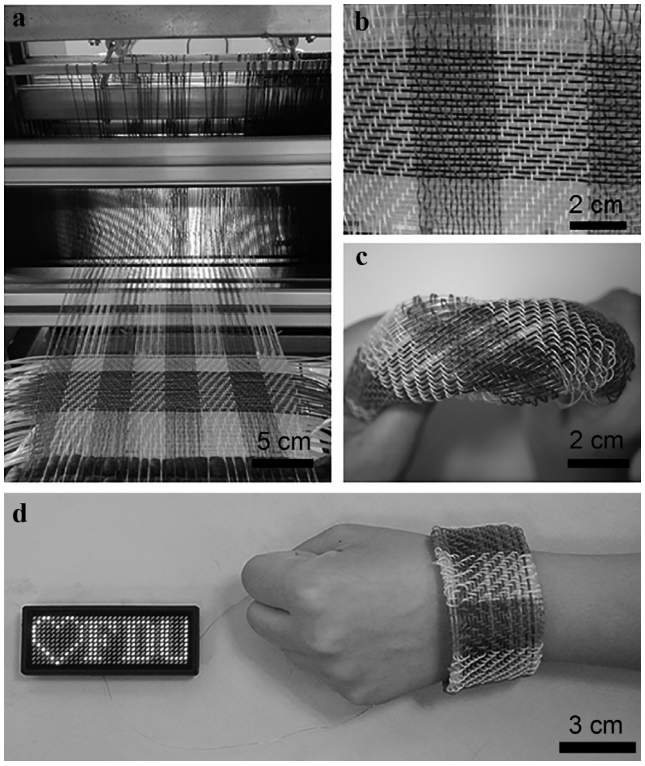

Figure 6. a) A photograph showing the progress of SOB fibers being woven into a textile. b,c) Photographs of the textile before and after twisting. d) The SOB textile lighting up an LED screen.

In conclusion, a new family of SOB fibers was created with high energy density and ultra-high flexibility, which had largely exceeded the other flexible batteries by up to 10 and 100 times, respectively. The SOB fibers had been further woven into flexible textiles, which is of importance for the booming market of portable and wearable electronics. This work offers a general and effective strategy for the development of high-performance energy storage devices.

Experimental Section

Synthesis of lithiated silicon/CNT hybrid fiber: Spinnable CNT arrays were first synthesized by chemical vapor deposition.[15] Aligned CNT sheets were continually pulled out of the spinnable CNT arrays. Silicon powder was dried in a vacuum oven at 80 °C overnight to remove water before use. 20 mg silicon powder was dispersed in *N*,*N*-dimethylformamide (20 mL) to obtain a suspension. The suspension was then evenly dropped onto the two stacked CNT sheet with width of 2 cm, followed by twisting into a silicon/CNT hybrid fiber. The hybrid fiber was assembled with a lithium sheet in a 2025-coin cell in glove box. 1 M LiTFSI dissolved in fluroethylene carbonate and tetraglyme (volume ratio of 1/4) was used as electrolyte. Celgard served as the separator while the Li sheet functioned as the counter electrode. After assembly, the battery was discharged and charged with a voltage range of 0.01 to 3 V at 0.1 mA for one cycle. Finally, the battery was discharged to 0.05 V at 0.1 mA and discharged to 0.01 V at 0.05 mA. After disassembled in glove box and rinsed by tetraglyme, lithiated silicon/CNT fiber was produced. To produce a longer lithiated silicon/CNT fiber, a silicon/CNT fiber was pre-lithiated in a glass bottle filled with electrolyte under the same condition.

Preparation of gel electrolyte: LiTFSI (0.2 M) and $LiNO_3$ (0.8 M) were first dissolved in 2 mL tetraglyme to form solution A. 1 g PVDF-HFP was dissolved in 4 g NMP to produce solution B. 0.01 g HMPP was added to 3 g TMPET to form solution C. Solutions A, B and C with weight ratios of 4/5/3 were first mixed to form a precursor solution and then exposed to UV light (wavelength of 365 nm) for 10 s to obtain a solidified and flexible gel electrolyte. All samples were processed and prepared in an argon-filled glove box.

Assembly of full battery: The lithiated silicon/CNT hybrid fiber was first coated with a layer of precursor solution, followed by exposure to UV irradiation (wavelength of 365 nm) for 10 s in an argon-filled glove box. The aligned CNT sheet with width of 1 cm were wrapped on the gel electrolyte-coated lithiated silicon/CNT fiber with a helical angle of 60°. The ratio of the weight of the lithiated silicon/CNT hybrid fiber anode and CNT cathode was 1.15/1. A punched heat shrinkable tube was finally used to seal the full battery.

Electrochemical measurement: The electrochemical measurements were conducted on an Arbin multichannel electrochemical testing system (MSTAT-5V/10 mA/16Ch). For the measurements of half cells, the lithiated silicon/CNT hybrid fiber was assembled with a lithium sheet in a 2025-coin cell in glove box. The specific capacity (C) was calculated by $C=(I\times t)/m$, where I, t and m represent the discharge current, discharge time and weight of lithiated silicon/CNT hybrid fiber, respectively. For the measurements of CNT cathode, the aligned CNT sheet with width of 1 cm were wrapped on the gel electrolyte-coated lithium wire with a helical angle of 60°. The half cells were placed in air with a relative humidity of 5%. The specific capacity (C) was calculated by $C=(I\times t)/m$, where I, t and m represent the discharge current, discharge time and weight of the CNT electrode, respectively. The SOB batteries were tested in air with a relative humidity of 5%. The specific capacity (C) was calculated by $C=(I\times t)/m$, where I, t and m represent the discharge current, discharge time and the weight of CNT electrode, respectively. The energy density (E) was calculated by $E=(I\times t\times V)/M$, where I, t, V and M represent the discharge current, discharge time, average discharge voltage and total weight of the two electrodes, respectively.

Acknowledgements

This work was supported by MOST (2016YFA0203302), NSFC (21634003, 51573027, 51403038, 51673043, 21604012) and STCSM (16JC1400702, 15XD1500400, 15JC1490200).

Conflict of interest

The authors declare no conflict of interest.

Keywords: batteries · carbon nanotube fibers · electrochemistry · energy storage · wearable electronic devices

How to cite: *Angew. Chem. Int. Ed.* **2017**, *56*, 13741 – 13746
Angew. Chem. **2017**, *129*, 13929 – 13934

[1] T.-H. Han, Y. Lee, M.-R. Choi, S.-H. Woo, S.-H. Bae, B. H. Hong, J.-H. Ahn, T.-W. Lee, *Nat. Photonics* **2012**, *6*, 105 – 110.
[2] G. S. Jeong, D.-H. Baek, H. C. Jung, J. H. Song, J. H. Moon, S. W. Hong, I. Y. Kim, S.-H. Lee, *Nat. Commun.* **2012**, *3*, 977.
[3] N. Li, Z. Chen, W. Ren, F. Li, H.-M. Cheng, *Proc. Natl. Acad. Sci. USA* **2012**, *109*, 17360 – 17365.
[4] H. Wu, Q. Meng, Q. Yang, M. Zhang, K. Lu, Z. Wei, *Adv. Mater.* **2015**, *27*, 6504 – 6510.
[5] L. Hu, F. La Mantia, H. Wu, X. Xie, J. McDonough, M. Pasta, Y. Cui, *Adv. Energy Mater.* **2011**, *1*, 1012 – 1017.
[6] M. Koo, K.-I. Park, S. H. Lee, M. Suh, D. Y. Jeon, J. W. Choi, K. Kang, K. J. Lee, *Nano Lett.* **2012**, *12*, 4810 – 4816.
[7] L. Wen, F. Li, H. M. Cheng, *Adv. Mater.* **2016**, *28*, 4306 – 4337.
[8] W. Liu, M. S. Song, B. Kong, Y. Cui, *Adv. Mater.* **2017**, *29*, 1603436.
[9] Y. Zhang, Y. Zhao, J. Ren, W. Weng, H. Peng, *Adv. Mater.* **2016**, *28*, 4524 – 4531.
[10] Z. Zhang, Y. Zhang, Y. Li, H. Peng, *Acta Polym. Sin.* **2016**, 1284 – 1299.
[11] H. Sun, Y. Zhang, J. Zhang, X. Sun, H. Peng, *Nat. Rev. Mater.* **2017**, *2*, 17023.
[12] J. Ren, Y. Zhang, W. Bai, X. Chen, Z. Zhang, X. Fang, W. Weng, Y. Wang, H. Peng, *Angew. Chem. Int. Ed.* **2014**, *53*, 7864 – 7869; *Angew. Chem.* **2014**, *126*, 7998 – 8003.
[13] Y. Zhang, Y. Wang, L. Wang, C.-M. Lo, Y. Zhao, Y. Jiao, G. Zheng, H. Peng, *J. Mater. Chem. A* **2016**, *4*, 9002 – 9008.
[14] Y. Zhang, W. Luo, C. Wang, Y. Li, C. Chen, J. Song, Y. Wang, L. Hu, *Proc. Natl. Acad. Sci. USA* **2017**, *114*, 3584 – 3589.
[15] W. Luo, Y. Zhang, S. Xu, J. Dai, E. Hitz, Y. Li, L. Hu, *Nano Lett.* **2017**, *17*, 3792 – 3797.
[16] Y. Zhang, L. Wang, Z. Guo, Y. Xu, Y. Wang, H. Peng, *Angew. Chem. Int. Ed.* **2016**, *55*, 4487 – 4491; *Angew. Chem.* **2016**, *128*, 4563 – 4567.
[17] S. Wu, K. Zhu, J. Tang, K. Liao, S. Bai, J. Yi, Y. Yamauchi, M. Ishida, H. Zhou, *Energy Environ. Sci.* **2016**, *9*, 3262 – 3271.
[18] B. Sun, X. Huang, S. Chen, P. Munroe, G. Wang, *Nano Lett.* **2014**, *14*, 3145 – 3152.
[19] X. Dong, L. Chen, X. Su, Y. Wang, Y. Xia, *Angew. Chem. Int. Ed.* **2016**, *55*, 7474 – 7477; *Angew. Chem.* **2016**, *128*, 7600 – 7603.
[20] M.-C. Lin, M. Gong, B. Lu, Y. Wu, D.-Y. Wang, M. Guan, M. Angell, C. Chen, J. Yang, B.-J. Hwang, *Nature* **2015**, *520*, 325 – 328.
[21] T. Liu, Q. C. Liu, J. J. Xu, X. B. Zhang, *Small* **2016**, *12*, 3101 – 3105.
[22] T. Liu, J. J. Xu, Q. C. Liu, Z. W. Chang, Y. B. Yin, X. Y. Yang, X. B. Zhang, *Small* **2017**, *13*, 1602952.

[23] Y. Zhang, Y. Zhao, X. Cheng, W. Weng, J. Ren, X. Fang, Y. Jiang, P. Chen, Z. Zhang, Y. Wang, *Angew. Chem. Int. Ed.* **2015**, *54*, 11177 – 11182; *Angew. Chem.* **2015**, *127*, 11329 – 11334.

[24] Y. H. Zhu, S. Yuan, D. Bao, Y. Yin, H. Zhong, X. Zhang, J. Yan, Q. Jiang, *Adv. Mater.* **2017**, *29*, 1603719.

Manuscript received: August 1, 2017
Revised manuscript received: August 25, 2017
Accepted manuscript online: September 20, 2017
Version of record online: October 2, 2017

